Electronic Supplementary Information (ESI)

Interaction between Positive and Negative Dielectric Microparticles / Microorganisms in Optoelectronic Tweezers

Shuzhang Liang[1,‡], Chunyuan Gan[1,‡], Yuguo Dai[1], Chaonan Zhang[1], Xue Bai[1], Shuailong Zhang[2,3], Aaron R. Wheeler[4,5,6], Huawei Chen[1,7,*], and Lin Feng[1,7,*]

[1]School of Mechanical Engineering & Automation, Beihang University, Beijing, 100191, China.

[2]School of Mechatronical Engineering, Beijing Institute of Technology, Beijing, 100081, China

[3]Beijing Advanced Innovation Center for Intelligent Robots and Systems, Beijing Institute of Technology, Beijing, 100081, China

[4]Department of Chemistry, University of Toronto, Toronto, Toronto, ON, M5S 3H6, Canada

[5]Institute of Biomedical Engineering, University of Toronto, Toronto, ON, M5S 3G9, Canada

[6]Donnelly Centre for Cellular and Biomolecular Research, University of Toronto, Toronto, ON M5S 3E1, Canada

[7]Beijing Advanced Innovation Center for Biomedical Engineering, Beihang University, Beijing, 100191, China

*Correspondence E-mail: chenhw75@buaa.edu.cn, linfeng@buaa.edu.cn

‡S. L. and C. G. contributed equally to this paper.

S1. Mathematical model of DEP force

A non-uniform electric field is induced by a light pattern to analyze DEP forces in a 2-dimension computational domain. The chamber walls and the particle are defined to be rigid and they are not conducive. The radius of the particle is represented by *r*. The particle is located nearby the light pattern. Owing to the diameter of the particle is more than 1μm and the temperature is equal to the room temperature, Brownian motion can be ignored in the manipulation of the OET system[1].

f_0 represents the potential applied to the light pattern in EF. In order to simplify the calculation, all physical quantities are considered dimensionless (the unit is 1). The number of charge densities is zero in the computational domain. Laplace equation is adopted to describe the electrical potential in the computational medium domain Ω, expressed as[2]:

$$\nabla_*^2 \phi^* = 0 \tag{1}$$

The electric field of domain Ω is:

$$E^* = -\nabla^* \phi^* \tag{2}$$

where, $\varphi^* = \phi_0$ at light pattern EF and $\varphi^* = 0$ at boundary AD.

The surfaces of sidewalls and particles are electrically insulating. Therefore, the relationship of electrical potential on surfaces Γ, AB, and DC can be expressed as:

$$\boldsymbol{n} \cdot \nabla^* \phi^* = 0 \tag{3}$$

For analyses of dipole moment in the electric field, the external field is equal to two source charges $+Q$ and $-Q$ with a distance of $2D$ (as shown in **Figure S1(a)**). Thus, the electric field intensity $E = Q/2\pi\varepsilon D^2$. The polarized charge ($q$) and the offset position (d) are expressed as[3,4]:

$$q = QR/D \tag{4}$$

$$d = R^2/D \tag{5}$$

where, R is the radius of the particle. Thus, the dipole moment (p) is expressed as:

$$p = 2qd = \frac{2QR^3}{D^2} = 4\pi\varepsilon R^3 E \tag{6}$$

When the particle is in a non-uniform electric field, it is necessary to use multiple dipoles to correct the dipole moment (as shown in **Figure S1(b)**). The effect multiple dipole moment (p_n) is expressed as:

$$p_n = \frac{1}{(2n-1)!!} 4\pi\varepsilon R^{2n+1} * {f_{CM}}^n * \nabla^{n-1} E \tag{7}$$

where, ε is the permittivities of particles. f_{CM} represents the Clausius-Mossotti factor.

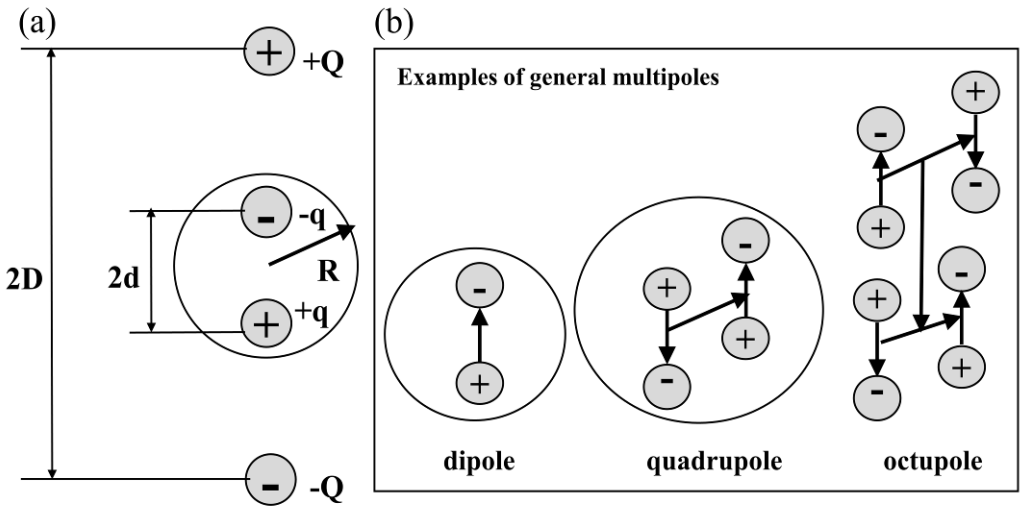

Figure S1. A dipole moment model of the particle in an OET device. (a) A dipole moment in the electric field. (b) Examples of multipoles inside particles.

Thus, the dielectrophoresis force is expressed as:

$$F = q * d * \nabla E(x) = p * \nabla E(x) \tag{8}$$

Then, the time-averaged DEP force can be expressed as[5]:

$$F = 2\pi R^3 \varepsilon_m Re[f_{CM}(\omega)] \nabla E_{rms}^2 \tag{9}$$

where, ε_m represents the permittivity of the medium and E_{rms} represents the root-mean-square (rms) value of the electric field strength. It is plural. Therefore, $Re[f_{CM}(\omega)]$ represents the real part of CM factor that mainly depends on the dielectric properties of particles and the suspending medium, expressed as:

$$f_{CM}(\omega) = \frac{\varepsilon_p^* - \varepsilon_m^*}{\varepsilon_p^* + 2\varepsilon_m^*} \tag{10}$$

where, ε_p* represents the complex permittivities of particles and ε_m* represents the complex permittivities of the suspending medium. The complex permittivity can be expressed as:

$$\varepsilon^* = \varepsilon - j\frac{\sigma}{\omega} \tag{11}$$

where, σ represents the electric conductivity of the object and ω represents the angular frequency of the alternating current (AC) source. j represents the imaginary unit. Therefore,

$$f_{CM}(\omega) = \frac{\omega(\varepsilon_p - \varepsilon_m) - j(\sigma_p - \sigma_m)}{\omega(\varepsilon_p + 2\varepsilon_m) - j(\sigma_p + 2\sigma_m)} \tag{12}$$

and

$$Re[f_{CM}(\omega)] = \frac{\omega^2(\varepsilon_p^2 + \varepsilon_p\varepsilon_m - 2\varepsilon_m^2) + (\sigma_p^2 + \sigma_p\sigma_m - 2\sigma_m^2)}{\omega^2(\varepsilon_p + 2\varepsilon_m)^2 + (\sigma_p + 2\sigma_m)^2} \tag{13}$$

where, σ_p represents the electric conductivity of particles and ε_p represents the permittivities of particles. σ_m represents the electric conductivity of the medium and ε_m represents the permittivities of the medium.

Therefore, the magnitude of DEP force mainly depends on the size of particles, the electric field gradient, and the electric property of particles, as well as the suspending medium. The direction of the DEP force depends on $Re[f_{CM}(\omega)]$. When the $Re[f_{CM}(\omega)]$ is larger than zero, the particles would be subjected to a positive DEP (pDEP would attract particles to the light spot); Otherwise, the particles would be subjected to a negative DEP (nDEP would repel particles from the light spot). **Figure S2(a)** presents the manipulated force of different microparticles in an OET device. The negative DEP acting on the particles at different positions is analyzed.

These particles are mainly subjected to two kinds of forces when they moving in the medium, in which the dielectrophoresis force $\boldsymbol{F}_E^*$ is generated from the electric field and the hydrodynamic force $\boldsymbol{F}_H^*$ is generated from the flow medium. The gravity and the buoyant

force are ignored, as shown in **Figure S2(b)**. Thus, the dielectrophoresis force $\boldsymbol{F}_E^*$ is also expressed as:

$$\boldsymbol{F}_E^* = \int (\boldsymbol{T}_E^* \cdot \boldsymbol{n}) d\Gamma^* = \int \left[\boldsymbol{E}^* \boldsymbol{E}^* - \frac{1}{2} (\boldsymbol{E}^* \cdot \boldsymbol{E}^*) \boldsymbol{I} \right] \cdot \boldsymbol{n} d\Gamma^* \tag{14}$$

where, $\boldsymbol{T}_E^*$ represents the MST on the particle surface which is Γ^*. n represents the unit vector.

The hydrodynamic force $\boldsymbol{F}_H^*$ can be expressed as:

$$\boldsymbol{F}_H^* = \int (\boldsymbol{T}_H^* \cdot \boldsymbol{n}) d\Gamma^* = \int [-p^* \boldsymbol{I} + (\nabla^* \boldsymbol{u}^* + (\nabla^* \boldsymbol{u}^*)^T] \cdot \boldsymbol{n} d\Gamma^* \tag{15}$$

where, $\boldsymbol{T}_H^*$ represents the hydrodynamic stress tensor. u^* represents the fluid velocity. On the ground that the fluid is laminar flow and Reynolds number is small in the OET system, the hydrodynamic stress tensor can be replaced by Stokes's drag force F_d^*. Stokes's drag force limits the movement of particles driven by DEP force. Stokes's drag force can be employed to measure the actual strength of DEP forces and the velocity of particles, expressed as:

$$\boldsymbol{F}_d^* = \frac{-6\eta A \boldsymbol{U}_P^*}{r} = -6\pi\eta r \boldsymbol{U}_P^* \tag{16}$$

where, the dynamic viscosity of the fluid ɦ is 1.0×10^{-3}kg/(m*s). $\boldsymbol{U}_\mathrm{p}^*$ represents the velocity of particles. $A = \pi R^2$ is the cross-sectional area of the particle.

As the experimental results, the microbeads moved at a maximum linear velocity of 21.56μm/s. According to the diameter of the object, the average diameter of the magnetic microspheres is 20 μm; therefore, the reference area is estimated as $A = \pi R^2 \approx 3.14\times100\times10\text{^}(-12)\ \mathrm{m}^2 = 3.14\times10\text{^}(-10)\ \mathrm{m}^2$. Thus,

$$F_d = \frac{6\eta A u}{r} \approx \frac{6\times1.0\times10^{-3}\times3.14\times10^{-10}\times21.56\times10^{-6}}{10\times10^{-6}} = 4.062\times10^{-12}N \tag{17}$$

The magnetic microspheres (diameter 20 μm) suffer a DEP force of 4.062 pN.

The E. gracilis moved at a maximum linear velocity of 15.03 μm/s. When applied the electric field, the E. gracilis is vertical in the microfluidic chip; therefore, the reference area is estimated as $A=l*d\approx 100\times 15\times 10\text{^} (-12)\ m^2=1.5\times 10\text{^}(-9)\ m^2=\pi R^2$. Thus,

$$F_d=\frac{6\eta Au}{r}\approx\frac{6\times 1.0\times 10^{-3}\times 1.5\times 10^{-9}\times 15\times 10^{-6}}{21.86\times 10^{-6}}=6.176\times 10^{-12}N \tag{18}$$

The E. gracilis suffer a DEP force of 6.176 pN.

The spirulina moved at a maximum linear velocity of 14.79 μm/s. When adding the electric field, the spirulina layed in the microfluidic chip, and the feature size of spirulina are 30 μm in diameter (D), 5μm in wire diameter (d), 100μm in the whole free length; therefore, the reference area is estimated as $A=\pi(R^2-r^2)\approx 3.14\times(15\times 15-10\times 10)\times 10\text{^}(-12)\ m^2=3.925\times 10\text{^}(-10)\ m^2$. Thus,

$$F_d=\frac{6\eta Au}{r}\approx\frac{6\times 1.0\times 10^{-3}\times 3.925\times 10^{-10}\times 14.79\times 10^{-6}}{11.18\times 10^{-6}}=3.115\times 10^{-12}N \tag{19}$$

The spirulina suffer a DEP force of 3.115 pN. According to the experimental results currently, this system is possible to generate the force up to several pN.

According to Newton's Second Law, then, the movement of the particles can be expressed as:

$$m_p^*\frac{d\boldsymbol{U}_p^*}{dt^*}=\boldsymbol{F}^*=\boldsymbol{F}_H^*+\boldsymbol{F}_E^* \tag{20}$$

where, $m_p{}^*$ represents the particle mess. Subsequently, the actual movement of particles can be expressed by center $\boldsymbol{x}_p{}^*$ as follows:

$$\boldsymbol{x}_p^*=\boldsymbol{x}_{p0}^*+\int_0^{t^*}\boldsymbol{U}_p^*dt^* \tag{21}$$

where, $\boldsymbol{x}_{p0}{}^*$ represents the beginning position before the movement of particles.

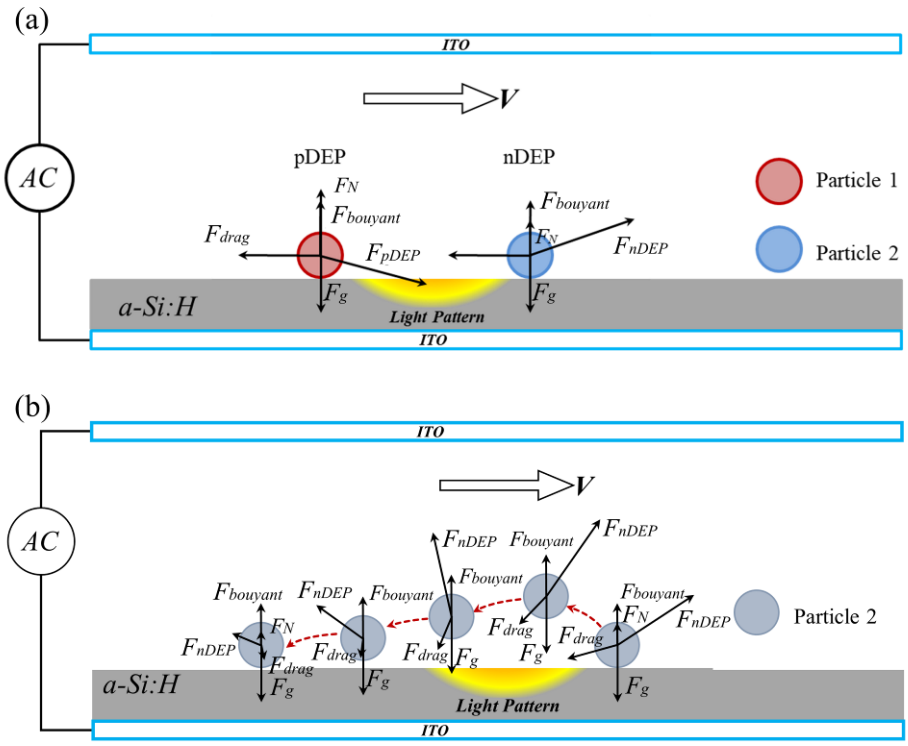

Figure S2. An analysis of the manipulated force of different microparticles in an OET device. (a) Particles subjected to negative DEP or positive DEP. (b) Particles subjected to negative DEP at different positions.

When multiple particles are placed in the electric field and the distance between two particles is close, these particles would interact with each other[6]. The mutual interaction can alter the local electric[7] field and induce mutual local DEP forces. To better understand this phenomenon, the dynamics of DEP particle-particle interactions have been examined in several studies [8-11]. A simple dipole model is used to analyze the interaction, as shown in **Figure S3**. The centers of symmetry of the two particles are neutral. When two particles interact, the force on the particles is the sum of the external electric field force and the mutual force. The total effect dipole moment is the sum of all the dipoles. It can be expressed as[12]:

$$p_e = -\sum_{n=1}^{\infty} 2\left(q_n d_n + q'_n d'_n\right) \tag{22}$$

Therefore, a particle can generate the dipole moment p, which can be expressed as[12]:

$$p_e = \beta a^3 \epsilon_f E_{loc} \tag{23}$$

where, $\beta = (\kappa\text{-}1)/(\kappa+2)$, $\kappa = \epsilon_p/\epsilon_f$ represents the ratio of the dielectric constant of particles and liquids, a represents the radius of particles, and d represents the distance between two interacted particles. With the adoption of a self-consistent method, the local electric field and electric potential can be expressed as:

$$u = -\frac{2\beta^2\epsilon_f a^6 {E_0}^2/d^3}{(1-\frac{4.8082\beta a^3}{d^3})^2} \tag{24}$$

$$E_{loc} = \frac{E_0}{1-4\beta a^3\zeta(3)/d^3} \tag{25}$$

where, $\zeta(3) = 1.20206$, and E_0 represents the external electric field strength. Under the action of the electric field, the two particles can be attracted along the z direction. By combining Equations (23) and (25), the interacted force of two particles can be expressed as:

$$f_{pair} = -\frac{6\beta^2\epsilon_f a^6 {E_0}^2/d^4}{(1-\frac{4.8082\beta a^3}{d^3})^2} \tag{26}$$

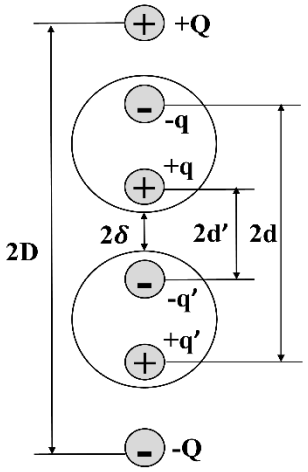

Figure S3. A simple dipole moment model of the interaction between two particles in an OET device.

Due to the attraction force between two particles relies principally on the range of κ, the mutual DEP force is determined by the specific dielectric properties of particles. As shown in **Figure S4**, we used the dipole moment to analyses the interaction between the particles. When the opposite side of the dipole is close, the two particles would be attracted (yellow

area). Otherwise, the two particles would be repelled when the same side of the dipole gets closely (blue area). It shows that the interaction effect on the same particles and the different particles is opposite in the same area. This would make the particles forming a different chain (a vertical chain or a horizontal chain).

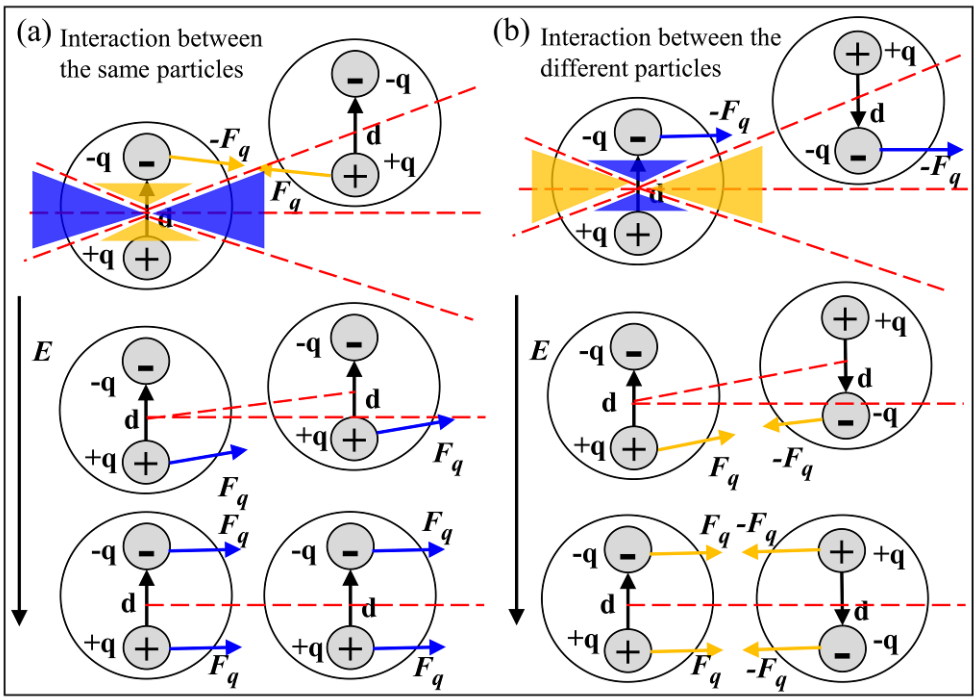

Figure S4. Image of the interaction process between two particles via a simple dipole moment model. (a) Interaction between the two same particles. (b) Interaction between the two different particles.

In the simulation model, the OET sandwich structure is used in COMSOL 5.5 model, as shown in **Figure S5(a)**. The depth of the fluid medium is 150μm. The ITO glasses layers are connected to the power supply. The voltage and frequency of the input signal are Φ_0=10V_{pp} and f=ω/(2π)=2 kHz, respectively. The density of the medium is set as ρ_f=1.0×10^{3}kg/m^3 and the viscosity of the medium is set as η=1.0×10^{3}kg/(m*s). In terms of the dielectric properties of the medium, the conductivity and permittivity are set as σ_f = 2.0×10^{-2}S/m and ε_f = 80, respectively. The DEP force acting on a particle can be positive or negative, due to the difference in electrical properties of the medium and particles, as shown in **Figure S5(b)** and **(c)**. With the adoption of different DEP forces in the OET system, the density of two kinds of

particles can be set as 1.05g/cm^3. The conductivity and permittivity of particle 1 driven by p-DEP force are s_p=0.2 S/m and e_p=2.56, respectively; those of particle 2 driven by n-DEP force are s_n=4.0×10^{-4} S/m and e_n=2.6, respectively. The different effects of dielectrophoretic force polarity on the particles in a non-uniform electric field are shown in **Figure S5(d)** and **(e)**, in which the respective trajectories of the particles reflect the attractive and repulsive effect of the light spot on the positive and negative particles, respectively.

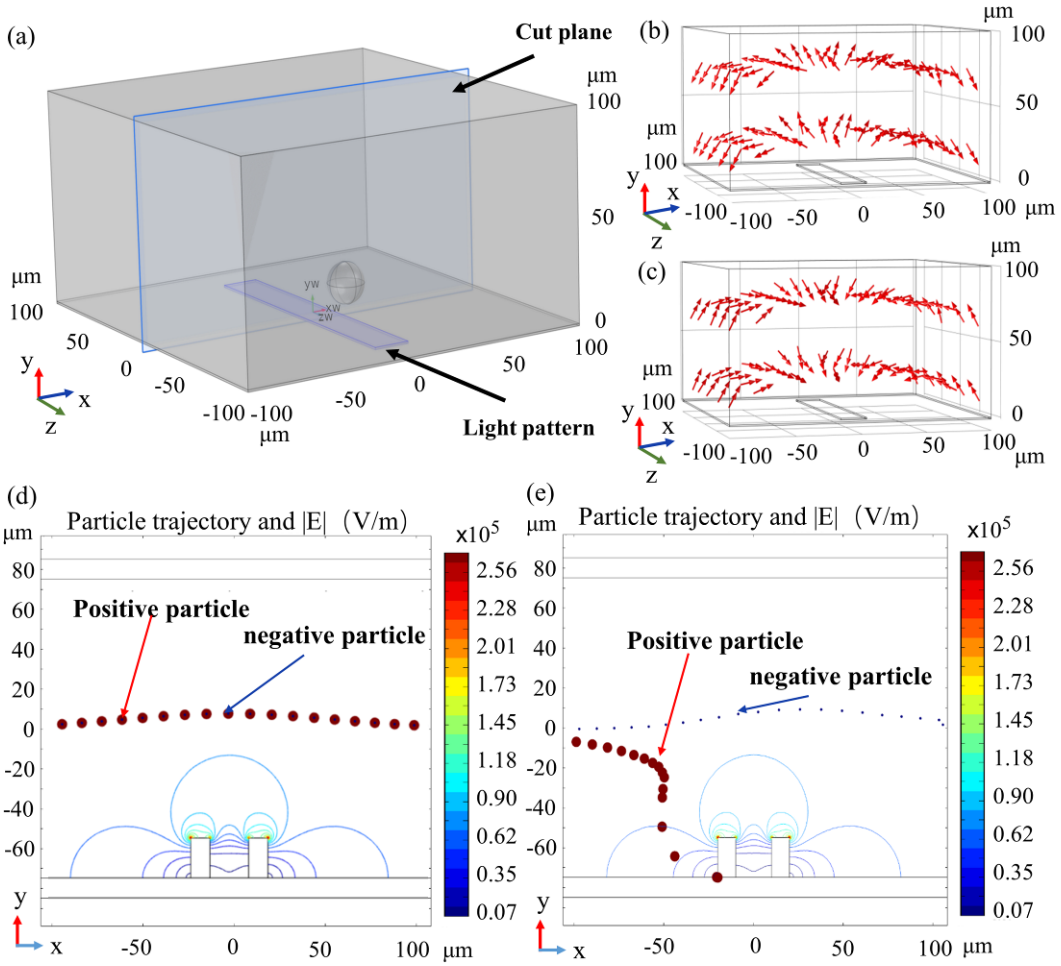

Figure S5. Simulation of DEP effect of different particles. (a) Illustration of the relative position of light pattern and particles in 3-Dimension model. (b) Simulation results show the n-DEP force vectors on a negative particle (particle 2) by the light pattern. (c) Simulation results show the p-DEP force vectors exerted on a positive particle (particle 1) by a light pattern. (d) Positive micro-object and negative micro-object do not separate in OET without the electric field. (e) Positive micro-object and negative micro-object separate in OET under the electric field.

S2. The force of a single particle influence by the frequency (*f*) of the power source

The frequency of the power source can be regarded as an initial parameter in the OET system. Manipulating a single particle can be changed by adjusting the frequency, which is a defined function related to the CM factor. Therefore, it can determine the direction of DEP force and the magnitude of force. In order to measure the DEP force exerted on particle 1 and particle 2, the frequency is changed from 1Hz to 10^{11}Hz individually, as shown in **Figure S6**. There is a sharp decrease from 9.457×10^{-14}N to -4.959×10^{-12}N in DEP force of particle 1 and the property of DEP force switches from "pull" to "push" between the frequency of 10^{6}Hz and 10^{8}Hz. As for particle 2, a smooth rise from -5.156×10^{-12}N to -4.968×10^{-12}N in DEP force can be noticed in the same frequency range. These tendencies in two particles are caused by the difference in conductivity (0.2S/m and $4*10^{-4}$S/m) changing the CM factor.

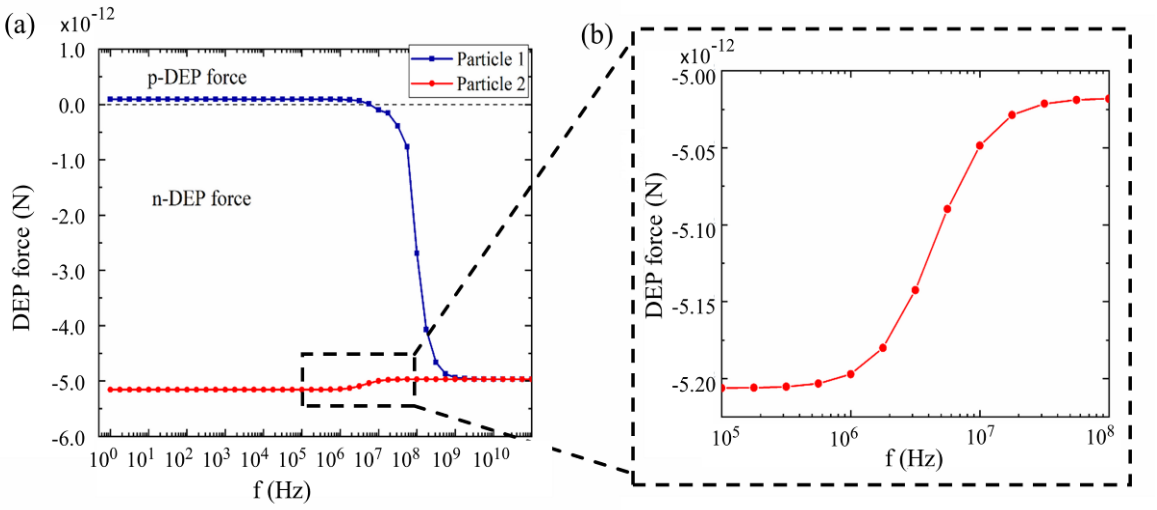

Figure S6. The relationship between DEP force and input frequency. (a) DEP forces of particle 1 (blue squares) and particle 2 (red dots), expressed as a function of AC frequency. p-DEP force is above the dotted line and n-DEP force is below the dotted line. (b) Partially enlarged view of DEP force changes in particle 2.

In this part, the polarization changing process is also used to explain the simulation results above. The dielectric will be charged due to an external electric field on the surface of particles (containing bound and free charges), as shown in **Figure S7**. The DEP force is generated from the charge that accumulates at the particle surface owing to polarization, known as the Maxwell-Wagner (MW) process[5]. The asymmetric distribution of positive and negative electric charges will also be affected by the original non-uniform electric field. Here,

electric polarization vector P is introduced to measure electric dipole moment density in particles. It is proportional to electric field intensity E, expressed as[13]:

$$P = \chi_e \varepsilon_0 E \tag{27}$$

where, χ_e represents the electric susceptibility. Therefore, P has the same direction as E.

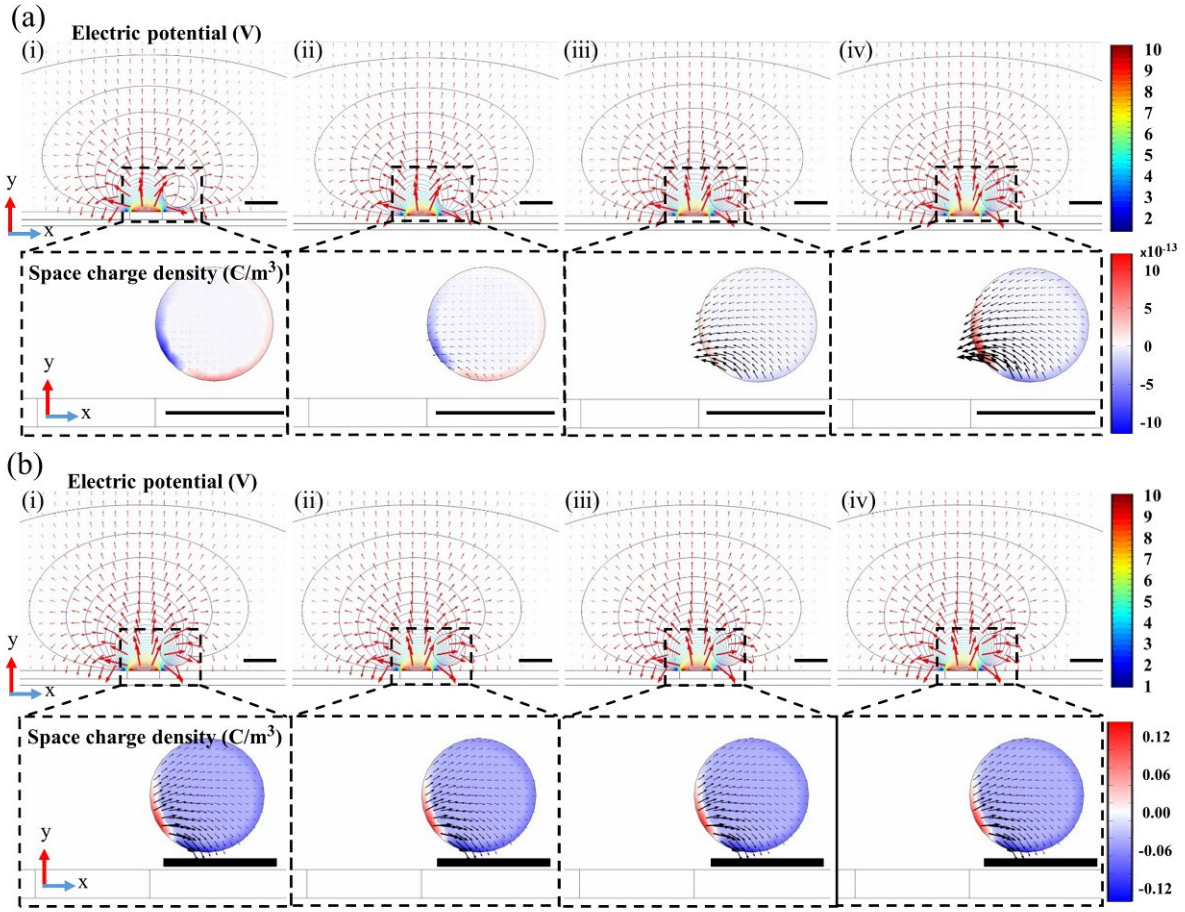

Figure S7. Simulations of potential distribution and space charge density of different particles with changes of the input frequency. (a) Simulated potential distribution (contour lines) and electric field (red arrows) of particle 1 with changes of the input frequency. Space charge density (blue and red part) and electric polarization vector P (black arrows) are shown in a partially enlarged view. AC frequencies of (i), (ii), (iii), and (iv) are 1Hz, 1.78×10^7Hz, 5.62×10^7Hz, and 1×10^{11}Hz, respectively. (b) Simulated potential distribution (contour lines) and electric field (red arrows) of particle 2 with changes of the input frequency. Space charge density (blue and red parts) and electric polarization vector P (black arrows) are shown in a partially enlarged view. AC frequencies of (i), (ii), (iii), and (iv) are 1Hz, 1.78×10^7Hz, 5.62×10^7Hz, and 1×10^{11}Hz, respectively. Scale bars are 20μm.

Thus, the electric field related to each point in space would be subjected to the force from electric charges according to Maxwell Theory. **Figure S7(a)** presents the distribution of

potential and electric field (red arrows) in the medium and particle 1 when a light pattern is projected on the OET chip. The length of red arrows represents the strength of the local electric field. When the power source frequency is low, it is obvious that the electric potential near a light pattern would be relatively high. Furthermore, the strength of the electric field in the medium is higher than that in particle 1 near the surface of particle 1. It is an electric field area with low strength inside particle 1. Positive and negative electric charges would be generated on the solid-liquid contact surface. The black arrows represent the polarization effect in particle 1 visually. Thus, electric dipole moment would emerge in particle 1. With the increase of frequency, the direction of polarization would change. In high frequency, particle 1 experiences n-DEP force rather than p-DEP force. As for particle 2 that experiences p-DEP force in the whole frequency range, the changes of DEP force are much fewer than that in particle 1. The mechanism can also be explained in **Figure S7(b)**. Due to a slight change in charges from 1Hz to 10^{11}Hz, the electric field almost remains unchanged, so that the DEP force changes a little.

S3. The force of a single particle influence by the voltage (V) of the power source

The voltage is closely connected with the electric field. **Figure S8(a)** presents the effect of voltage on DEP forces in particle 1 and particle 2. The force of both particle 1 and particle 2 is in an upward trend with the increase of the voltage. The ascent velocity of particle 2 is much higher than that of particle 1. The different changes of DEP forces would occur on account of the distribution of the electric field and polarization in the particles, as shown in **Figure S8(b)** and **(c)**. The outer electric field would induce polarization inside the particle and the moving charges would affect the electric field in turn. Here, the DEP force of particle 1 is

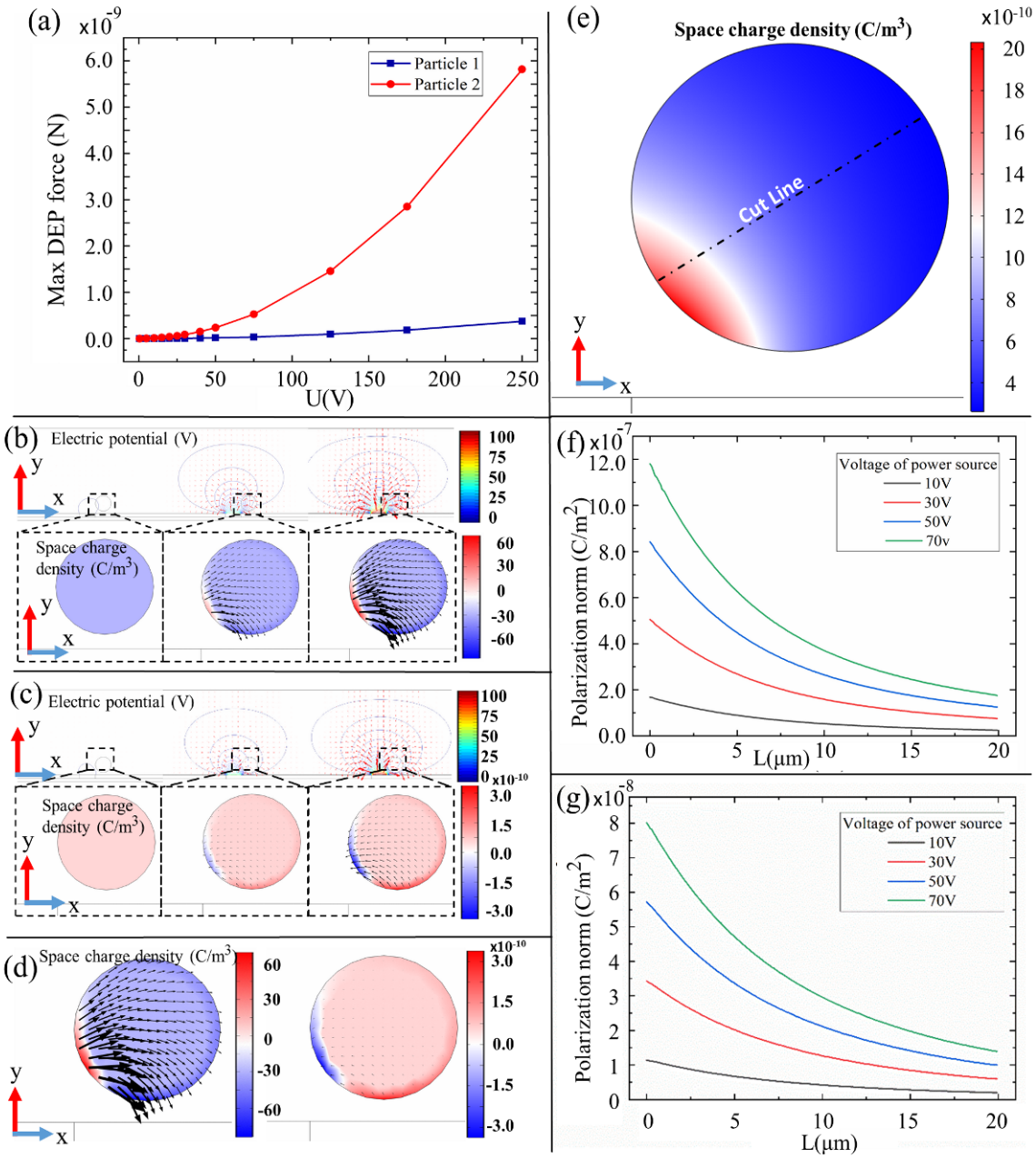

Figure S8. The relationship between DEP force and input voltage. (a) DEP forces of particle 1 (blue squares) and particle 2 (red circles), expressed as a function of the voltage of power source. (b) Simulated potential distribution (contour lines) and electric field (red arrows) of particle 2 when the voltage is 1V, 50V, and 100V, respectively. (c) Simulated potential distribution (contour lines) and electric field (red arrows) of particle 1 when the voltage is 1V, 50V and 100V, respectively. Space charge density (blue and red parts) and electric polarization vector P (black arrows) are shown in a partially enlarged view. (d) Space charge density (blue and red parts) and electric polarization vector P (black arrows) of particle 1(left) and particle 2(right) when the voltage is 100V. The diameter of particles is 20μm. (e)The polarization and the cut line position of particle 1. (f)The distribution of polarization norm along the cut line of particle 2. (g)The distribution of polarization norm along the cut line of particle 1. The diameter of these particles is 20μm.

larger than that of particle 2 in that the conductivity and permittivity differ in the polarization inside particles, as shown in **Figure S8(d)**. The directions of polarization vector P are opposite in two particles, which indicates that the directions of DEP forces are also different. Polarization density is used to analyze the DEP forces. As shown in **Figure S8(e)**, the particle part near the light pattern is exposed to a higher polarization density than the farther part. It means that the particle generates a multipole moment effect in this non-uniform field. **Figure S8(f) and (g)** present the data of polarization density along the cut line of particle 1 and particle 2. These show that the polarization will increase largely with the increase of the voltage, and it would result in larger DEP forces shown in Figure S8(a).

S4. The DEP force influence by the conductivity and permittivity of the medium

The conductivity and permittivity of the medium are also regarded as initial parameters of the medium that affect DEP forces. **Figure S9(a)** and **(b)** present the effect of the conductivity of the medium on the DEP forces of particle 1 and particle 2. Both particles would be subjected to p-DEP forces first and then n-DEP forces. These two particles will experience a turning point where DEP force is 0 as the conductivity goes up, due to the conductivity of the medium and particles is equal at this point. When the conductivity of the medium is relatively lower than that of particles, particles will be subjected to the p-DEP force. There would be an electric field area with low strength inside the particle, and the distribution of charges indicates that particles are subjected to the p-DEP force. It should be noted that the maximum n-DEP force is much larger than the maximum p-DEP force. The colored band in Figure S9(a) and (b) represent the same conductivity range. The increase in red and blue bands is caused by a large change in the electric field. However, the electric field would be subjected to dramatic changes near the turning point, as shown in **Figure S9(c)** and **(d)**. There is a slight change in the polarization when the conductive of the medium is far away from the turning point. The

polarization density of particle 1 and particle 2 along the cut line is shown in **Figure S9(e)** and **(f)**. Otherwise, there is a large change in polarization density around the turning point, which would result in a change in the direction and the strength of DEP forces.

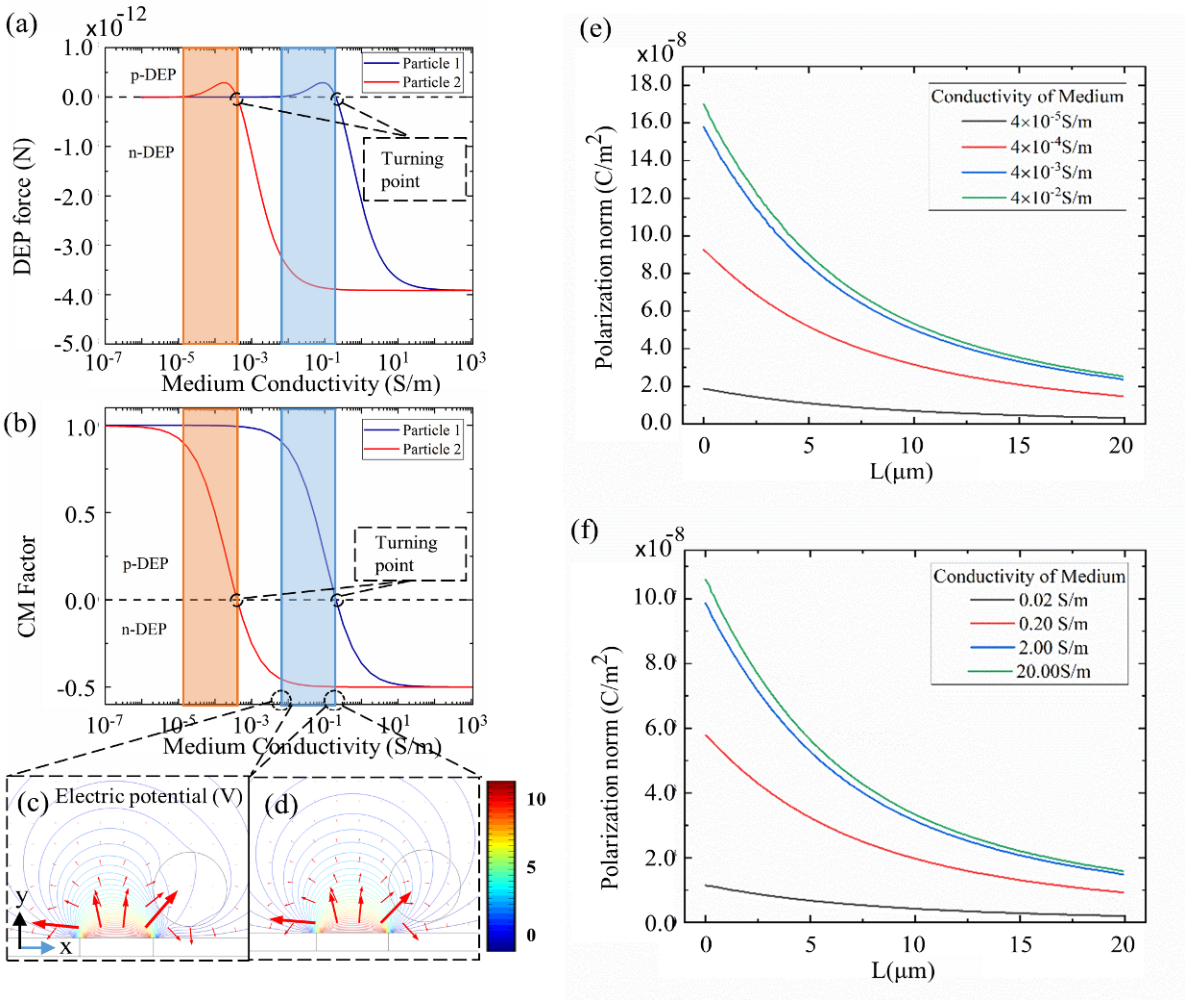

Figure S9. The relationship between DEP force and medium conductivity. (a) DEP forces of particle 1(blue) and particle 2(red), expressed as a function of the conductivity of the medium. (b) CM factors of particle 1(blue) and particle 2(red), expressed as a function of the voltage of conductivity of the medium. (c-d) Simulated potential voltage distribution (contour lines) and electric field (red arrows) of particle 1 when the conductivity of medium is 0.01S/m and 0.2S/m, respectively. The diameter of these particles is 20μm. (e) The distribution of polarization norm along the cut line of particle 2 in different medium conductivity. (f) The distribution of polarization norm along the cut line of particle 1 in different medium conductivity.

In addition, **Figure S10** also presents the DEP effect of the permittivity of the medium. The DEP force is proportional to the permittivity of the medium in case that the voltage is constant and AC frequency is 2kHz. However, the permittivity could exert slight impacts on the

electric field, which would remain almost the same in the simulation process. Then, several common media are selected to analyze the medium effect on the DEP force of different particles, as shown in **Figure S10(b)**. It shows that we need to configure high permittivity and low conductivity solutions that could induce enough DEP force to manipulate particles.

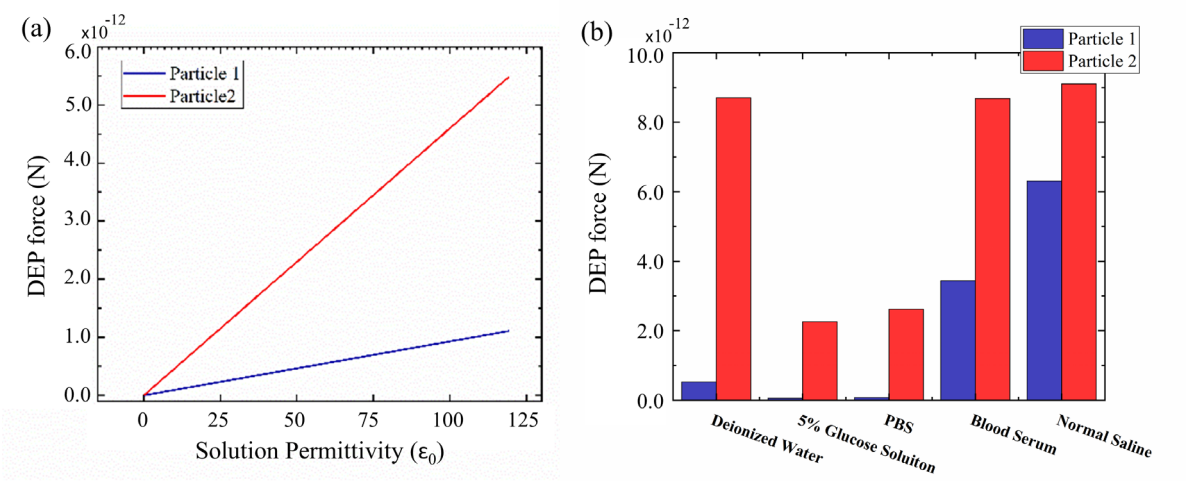

Figure S10. The relationship between DEP force and medium conductivity. (a) DEP forces of particle 1(blue) and particle 2(red), expressed as a function of permittivity of the medium. (b) DEP forces of particle 1 and particle 2 in different media.

S5. The Effects of input power on the interaction between two particles.

An effect of external input signals on particle interactions is shown in **Figure S11(a) and (b)**. In this experiment, the distance between two particles was set as 30μm and the input voltage was set as $10V_{pp}$. The input frequency was charged from 1Hz to 10^{11}Hz. According to Newton's Third Law, the interacted forces between both particles are equal in magnitude and opposite in direction. The DEP force of particle 1 was measured. In terms of the interaction between two particles with different dielectric properties, the DEP force has the opposite direction as a p-DEP force in the low-frequency range (from 1Hz to 10^6Hz) and n-DEP force in the high-frequency region (beyond 10^{10} Hz). There is a sharp decrease from 1.269×10^{-11}N to -1.096×10^{-11}N in the DEP force of particle 1, which shows that the property of DEP force switches from “attract” to “repel” between frequencies of 10^6Hz and 10^8Hz. In terms of the

interaction between two particles with the same dielectric properties, the DEP force decreases from -1.167×10^{-11}N to -1.096×10^{-11}N in the same frequency range (from 10^{6}Hz to 10^{8}Hz). The changing frequency and electric parameters result in the changes of the CM factor which defines the direction and magnitude of DEP force. Because the conductivity of particle 2 is much smaller than that of particle 1, the interaction force between particle 1 and particle 2 is larger than that between particle 2 and particle 2 in the low-frequency range.

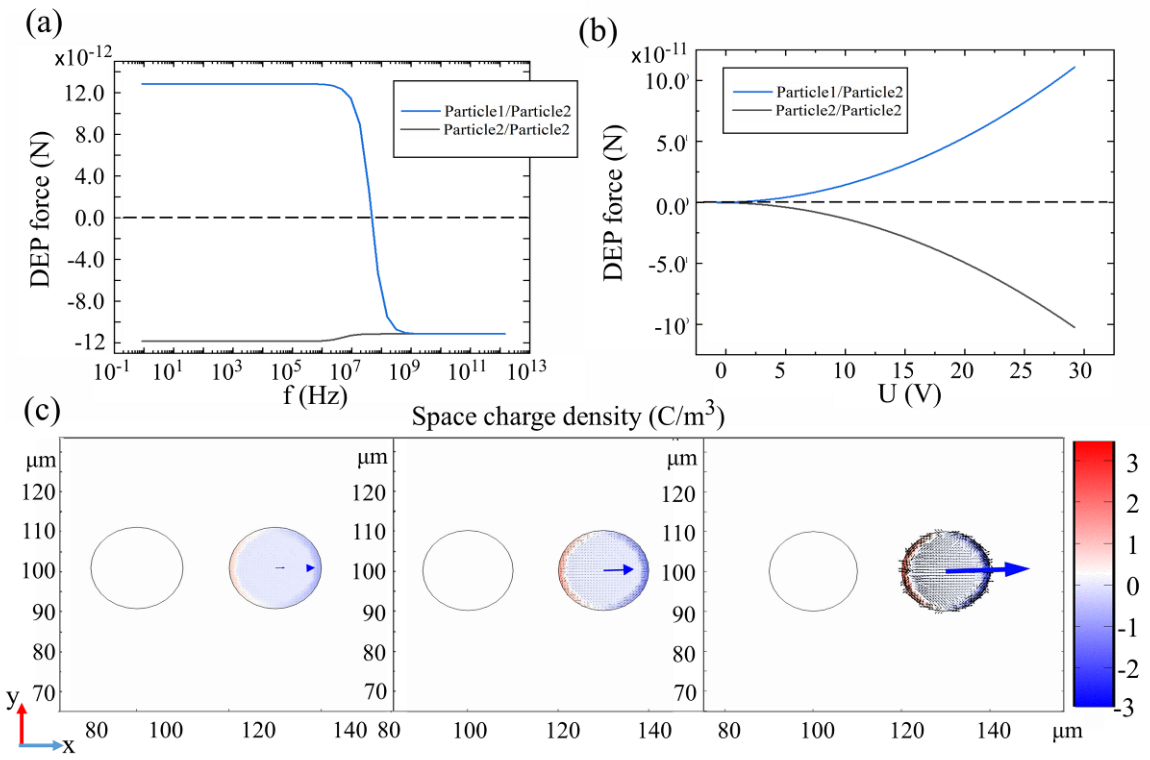

Figure S11. Effects of input power on the interaction between two particles. (a) The relationship between DEP force and input frequency. (b) The relationship between DEP force and input voltage. (c) The distribution change of space charge density of the particle with the increase of the input voltage.

According to the theoretical formula of DEP forces in the OET, the force is positively proportional to the square of the electric field intensity. Figure S11(b) presents the effect of voltage on DEP forces under the interaction of particles. In this simulation, the distance between two particles was set as 30μm and the input frequency was set as 2kHz. The difference is that the direction of forces is opposite in two different particles. Then, the space

charge density polarized in the particle would also show the voltage effect, as shown in **Figure S11(c)**. The polarization vector P (blue arrow) represents the increased DEP forces.

S6. The microfluidic chip and OET system

The OET chip is fabricated as a sandwich structure, which is composed of the indium-tin-oxide (ITO) glasses, aqueous solution, and indium-tin-oxide (ITO) glasses coated with a photoconductive thin film layer, as shown in **Figure S12(a)**. Subsequently, the chip is integrated into the OET platform, as shown in **Figure S12(b)**, which is employed to manipulate microparticles and microorganisms with opposite dielectric properties and different sizes and dimensionalities.

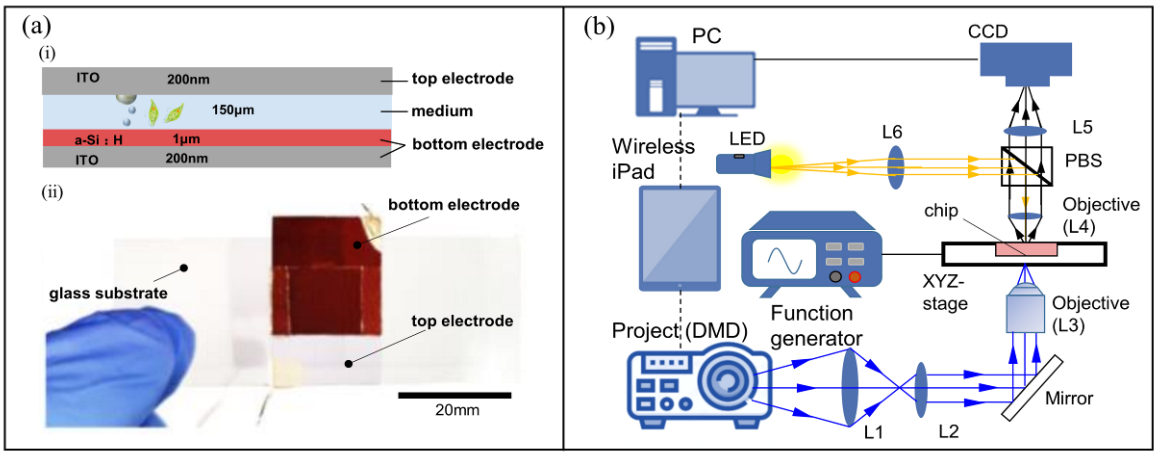

Figure S12. Simple OET system and a-Si microfluidic chip. (a) Structure of fabricated a-Si microfluidic chip. (b) Schematic of installed OET system with a microfluidic chip. Image projection path through lenses L1, L2, and objective lens and reflection from mirror. L4, PBS, L5, and CCD comprise the observation path; LED, L6, PBS, and L4 comprise the illumination path.

S7. Image identification for wireless control

There are two methods designed for two distinct operational situations. In terms of the situation in which the targeted particles have regular round contours, a pattern extraction approach can be applied, through which key contour features can be extracted through preprocessing procedures, including graying, blurring, and binarization, and the coordinates

can be determined with a Hough circle transformation. For the situation in which the objects are irregular particles, a pattern match method involving the application of graying can be adopted.

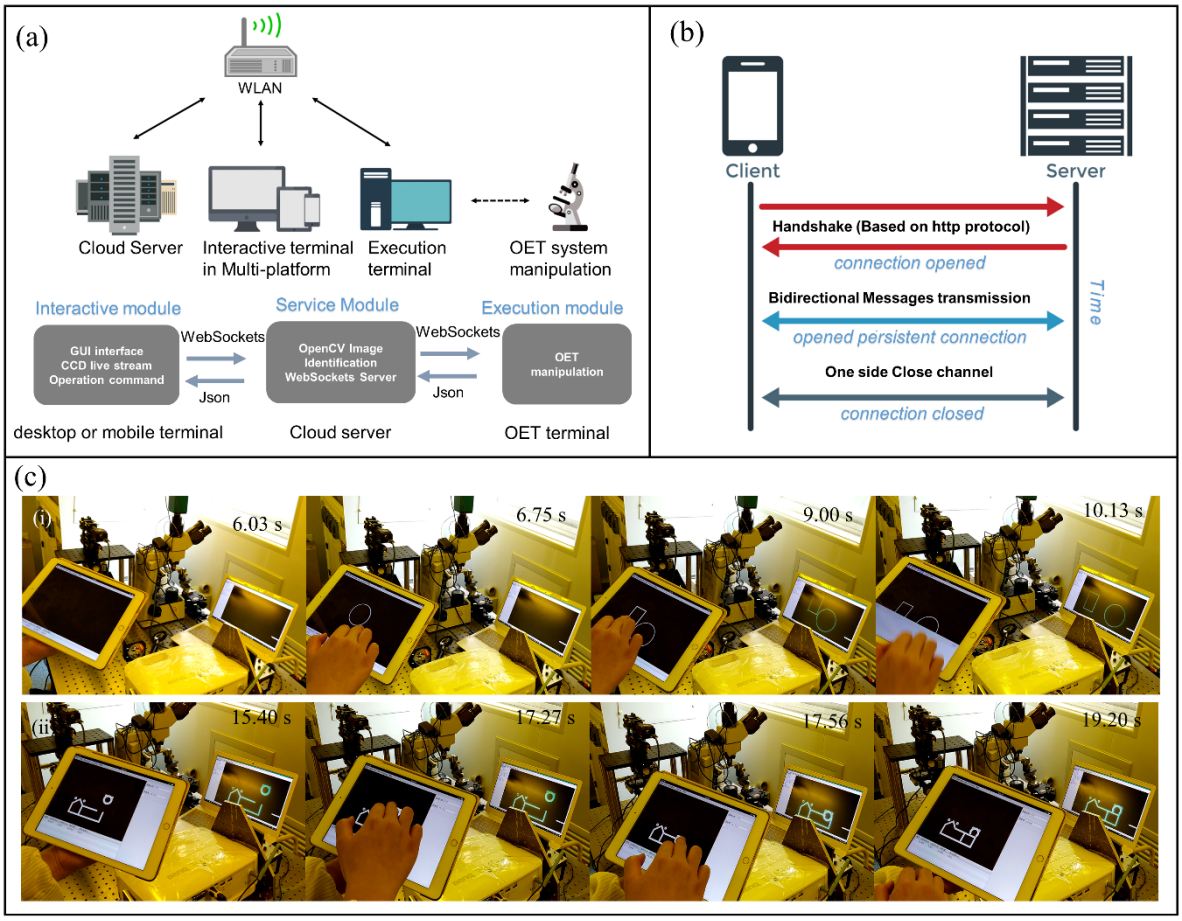

Figure S13. OET control system display and data server transmission principle. (a) Cloud data transmission via WebSockets. (b) Schematic and model of Cloud-based wireless control. (c) Wireless-control display in fixed- and free-control modes.

The scheme of the Cloud-based wireless-control platform is shown in **Figure S13(a)**. The platform is composed of a Cloud server, multi-platform interactive terminals, and an executive terminal including the OET equipment. The three modules are deployed under a wireless local area network and could conduct safe communication based on the WebSocket protocol. The wireless-data transmission principles are shown in **Figure S13(b).** The wireless control platform separates various OET functions into different modules; the efficiency and specialization of the system can be enhanced by performing complicated centralized data

processing within the high-performance Cloud server. The operation of the Cloud wireless control system via iPad is shown in **Figure S13(c)** and the projected pattern is designed with the iPad GUI and sent via the Cloud server to the executive terminal computer. **Movie 8** presents the wireless control process of OET via the interactive iPad GUI.

S8. Supplementary Movies:

Movie S1. Simulation of the different dielectric property particles suffered the DEP effect under the same non-uniform electric field.

Movie S2. Simulation and experiment of the light moving to manipulate particles in the OET.

Movie S3. Simulation of the distribution of space charge density of the two microparticles when the positive particle interacts with the negative particle in different positions.

Movie S4. Simulation and experiment of two microparticles in the interaction process.

Movie S5. Controlled positive dielectric micro-object to interact with multiple negative dielectric microparticles via OET.

Movie S6. Positive dielectric swimming euglena gracilis interact with micro-objects via optoelectronic tweezers. The polystyrene microbeads are adhered to the Euglena gracilis and transported by euglena gracilis.

Movie S7. Positive dielectric micro-spirulina interact with negative dielectric micro-object transportation via optoelectronic tweezers.

Movie S8. Wireless control display through the iPad interaction interface in the OET platform.

S9. Supplementary References:

1. A. N. Borodin and P. Salminen, *Brownian Motion*, Birkhauser, 1996.
2. Y. Ai, A. Beskok, D. T. Gauthier, S. W. Joo and S. Qian, *Biomicrofluidics*, 2009, **3**, 210.
3. T. B. Jones, *Journal of Applied Physics*, 1986, **60**, 2226-2230.
4. T. B. Jones, *Cambridge Univ Pr*, 1995.
5. T. Jones, *Electromechanics of particles.Cambridge University Press*, 1995.
6. L. Liu, C. Xie, B. Chen and W. U. Jiankang, *Applied Mathematics and Mechanics*, 2015, **36**, 1499-1512.
7. V. S. F. Klingenberg D J , Zukoski C F . , *The Journal of Chemical Physics*, 1989, **91**, 7888.
8. A. Ye and S. Qian, *Journal of Colloid & Interface Science*, 2010, **346**, 448-454.
9. A. T. J. Kadaksham, P. Singh and N. Aubry, *Electrophoresis*, 2004, **25**, 3625-3632.
10. M. Janjua, S. Nudurupati, I. Fischer, P. Singh and N. Aubry, *Mechanics Research Communications*, 2009, **36**, 55-64.

11. R. Tao, Q. Jiang and H. K. Sim, *Physical Review E Statistical Physics Plasmas Fluids & Related Interdisciplinary Topics*, 1995, **52**, 2727-2735.
12. R. Tao, Q. Jiang and H. K. Sim, *Physical Review E Statistical Physics Plasmas Fluids & Related Interdisciplinary Topics*, 1995, **52**, 2727.
13. Z. R. Gagnon, *Electrophoresis*, 2011, **32**, 2466-2487.